Spatially Partitioned Robust Optimization for Energy-Efficient Underwater Wireless Sensor Networks under Simulation-Informed Network Conditions

Ozhan Eren and Aysegul Altin-Kayhan
Department of Industrial Engineering
TOBB University of Economics and Technology
Ankara, Turkiye
e-mail: {ozhaneren | aaltin}@etu.edu.tr

***Abstract*—Underwater Wireless Sensor Networks (UWSNs) have attracted considerable attention for decades, owing to their broad spectrum of application areas. Despite technological advances, designing energy-efficient underwater communication architectures remains a key challenge due to the harsh and dynamic environment. Among the various factors influencing the performance of UWSNs, data traffic load emerges as a critical component, particularly in relation to the operational lifetime. Additionally, with their increasing deployment, Autonomous Underwater Vehicles (AUVs) are integrated into UWSNs in various roles. However, their presence introduces new challenges that require the design of robust sensor network configurations capable of effectively detecting and interacting with AUVs. This paper addresses a novel simulation-driven and uncertainty-aware design scheme for energy-efficient UWSNs. Building on prior studies of data traffic uncertainty in wireless sensor networks and AUV mobility, this paper employs a simulation environment that captures the integrated interactions among mobile targets, sensor nodes, and seabed topography to evaluate the proposed network model. Furthermore, recognizing that the unrestricted mobility of navigating vehicles can cause variations in data generation rates across the network, we apply balanced 3D K-means partitioning to structure the network for uncertainty modeling. The proposed robust optimization framework is evaluated against a deterministic baseline under varying traffic conditions induced by vehicle movement. To capture uncertainty at multiple scales, we incorporate parameters representing sensor-specific deviations and regional conservativeness, enabling examination of their impact on solution stability. Results indicate that the robust framework consistently outperforms the deterministic approach across varying levels of traffic deviation under the applied spatial partitioning scheme.**

***Keywords*-Simulation; spatial partitioning; underwater wireless sensor networks; traffic uncertainty; robust optimization.**

I. INTRODUCTION

Underwater Wireless Sensor Networks (UWSNs) have become essential for diverse underwater applications, including environmental monitoring, offshore exploration, scientific investigation, and marine operations involving submarine detection, AUV-assisted monitoring, and maritime observation for situational awareness [1]–[4]. Comprising spatially distributed acoustic sensor nodes, UWSNs are designed to observe and transmit underwater phenomena to a base station, often through multi-hop communication schemes. Due to the inherent challenges in accessing and replacing deployed sensor nodes, energy efficiency is a critical design consideration.

Recent advancements in underwater acoustic communication and the integration of heterogeneous underwater platforms have significantly expanded the capabilities of UWSNs. Nevertheless, these networks still face persistent operational challenges, especially in dynamic and mission-oriented environments. The need to detect and track mobile entities such as submarines and AUVs creates sensing demands that vary spatially and temporally. As these entities move through the monitored area, nearby nodes experience fluctuating sensing activity, resulting in uneven data generation and shifting traffic patterns. Such imbalances result in localized energy depletion, reduced network availability, and premature degradation of system performance [5]. Therefore, understanding how target mobility affects sensing dynamics and communication load is crucial for developing resilient UWSNs.

Our primary goal is to design an event-driven UWSN capable of monitoring a designated underwater area through a robust optimization approach. For a comprehensive literature review on the topic, the interested reader is referred to [6], where a preliminary formulation was introduced to address uncertainty using a global robustness framework. Building upon this foundation, the current study extends the analysis by incorporating spatial heterogeneity through a region-based modeling strategy. To better capture spatial variability in uncertainties, we partition the 3D underwater network into sub-regions, allowing region-wise deviations for detailed analysis of localized uncertainties. Several spatial partitioning methods, such as grid-based schemes, clustering algorithms, and Voronoi tessellations, have been explored in underwater studies [7]–[9]. In this study, we adopt a balanced 3D K-means clustering approach to achieve spatial division that reflects the structure and operational characteristics of underwater environments. This method provides a practical and effective means to form spatially compact and evenly sized regions, facilitating the application of localized deviation scenarios and enabling clearer analysis of their region-specific impacts on network behavior [10].

More specifically, we address the problem of minimizing the maximum initial battery allocation to sensors while ensuring sustained network operation over a specified time period. The robust design framework determines energy allocations that remain feasible across all admissible data rate variations, guided by a reference lifetime defined during the configuration phase. In contrast, the nominal design which does not consider uncertainty may lead to premature network failure under slight deviations from expected sensing rates. Subsequent evaluation shows that the robust design consistently achieves network lifetimes at or near the reference lifetime, demonstrating improved resilience and reliability compared to the nominal ap-

proach.

Finally, we present detailed analyses illustrating the performance of both robust and deterministic designs during the implementation phase, based on comprehensive tests conducted across a wide range of scenarios.

The major contributions of this study are as follows:

- We utilize a comprehensive simulation framework that integrates underwater vehicle movements, sensor deployment, and detailed seabed topography derived from real-world bathymetric data. This allows realistic estimation of sensing rates as they vary with sensor locations and target trajectories, forming a critical input for our robust model.
- We introduce a novel robust optimization framework for UWSNs featuring balanced 3D K-means spatial partitioning. This approach captures localized uncertainty and traffic load variations more precisely, enhancing the network's resilience and performance.
- We present comprehensive test results on the performances of the nominal design made without considering the uncertainty in the configuration phase and the robust design under a polyhedral uncertainty definition in different sensing rate scenarios when they are put into practice. The test results indicate that minor variations in sensing rates substantially impair the performance of the deterministic design, whereas the robust design consistently preserves the expected performance and extends operational longevity relative to the deterministic approach.

The remainder of this paper is organized as follows. Section II presents the main components of our optimization framework. We begin by introducing an optimization model for the deterministic design of underwater networks in Section II-A, followed by the robust counterpart formulation that enables analysis under uncertainty in Section II-B. Section II-C then describes the simulation environment used to derive sensor data generation rates. Computational results and performance analysis are provided in Section III, organized around the configuration and implementation phases. Finally, Section IV concludes the study with a summary and directions for future research.

II. Problem Definition

A. The Network Model

In this section, we will first present the classical mathematical model for the problem of efficient energy allocation to sensors. Next, we will block out how we integrate the uncertainty in detection rates into the model within the framework of robust optimization. In all models, we assume that the sensors and sink possess all the necessary capacity to process the data that they are supposed to transmit and receive, respectively. As indicated in [11] and [12], we consider only transmitting and receiving energy consumption, which are dominant with respect to other forms of consumptions like sensing and processing. The channel characteristics are considered ideal and the number of retransmissions due to failures is negligible [13]. We present the notation used in the paper in Table I.

Given the data sensing rates of the sensors, the following mathematical model ($E^{\text{det}}_{\max}$) aims to determine the initial energy allocations for the sensors, which ensures the energy-efficient operation of the network over default network lifetime T:

TABLE I. Sets, parameters, and decision variables.

Sets	
N	Set of sensor nodes
N_G	Set of all nodes in the network, i.e., $N \cup \{\text{BS}\}$, where BS denotes the base station
$\mathscr{R}$	Set of sensor subsets (regions), i.e., $\mathscr{R} = \{R_1, R_2, \dots\}$ with $R_j \subseteq N$
R_j	A subset of sensors forming region R_j, i.e., $R_j \in \mathscr{R}$
$\mathscr{J}$	Index set of regions, i.e., $\mathscr{J} = \{1, 2, \dots, \lvert\mathscr{R}\rvert\}$
$\mathscr{S}$	Set of sensing rate vectors within feasible intervals satisfying regional sum constraints
A	Set of directed one-hop connections: $A = \{(i,j) : i \in N, j \in N_G \setminus \{i\}, d_{ij} \leq R\}$
G	Directed graph repesenting the network, i.e., $G = (N_G, A)$
$\mathscr{U}$	Uncertainty set of feasible sensing rate vectors
Parameters	
d_{ij}	Euclidean distance between $i \in N$ and $j \in N_G$
T	Default network lifetime in configuration
R	Transmission range for sensors (m)
e^{TX}_{ij}	Energy cost of transmission from $i \in N$ to $j \in N_G$ per bit (mJ/bit)
e^{RX}_{ji}	Energy cost of reception by $i \in N$ from $j \in N$ per bit (mJ/bit)
s_k	Sensing rate of sensor $k \in N$ (bit/s)
s^k_{nom}	Nominal sensing rate of sensor $k \in N$ (bit/s)
s^k_{dev}	Sensing rate deviation of sensor $k \in N$ (bit/s)
α	Regional uncertainty budget
β_{kj}	Binary parameter indicating whether sensor k belongs to region R_j, where $j \in \mathscr{J}$
Variables	
f^k_{ij}	Proportion of s_k sensed by $k \in N$ transmitted on $(i,j) \in A$
e_i	Initial energy to be allocated to $i \in N$ (mJ)
$e^{\text{rob}}_{\max}$	Maximum energy assigned to a sensor in N under the robust model (mJ)
$e^{\text{det}}_{\max}$	Maximum energy assigned to a sensor in N under the deterministic model (mJ)
μ_{ik} , λ_{ik}	Deviation duals
θ_{ji}	Regional budget dual variable

$$min \quad e^{\text{det}}_{\max} \tag{1}$$

$s.t.$

$$\sum_{(i,j)\in A} f^k_{ij} - \sum_{(j,i)\in A} f^k_{ji} = \begin{cases} 1 & \text{if } i = k \\ -1 & \text{if } i = BS \\ 0 & \text{otherwise} \end{cases}$$
$$\forall i \in N_G,\ k \in N \tag{2}$$

$$\sum_{k\in N} \left[\sum_{(i,j)\in A} Te^{TX}_{ij} f^k_{ij} s_k + \sum_{(j,i)\in A} Te^{RX}_{ji} f^k_{ji} s_k \right]$$
$$\leq e_i \qquad \forall i \in N \tag{3}$$
$$e^{\text{det}}_{\max} \geq e_i \qquad \forall i \in N \tag{4}$$
$$f^k_{ij} \geq 0 \qquad \forall (i,j) \in A,\ k \in N \tag{5}$$
$$e_i \geq 0 \qquad \forall i \in N \tag{6}$$

B. The Network Model for Polyhedral Sensing Rates

The polyhedral uncertainty model is widely adopted in robust optimization due to its favorable balance between computational efficiency and strong worst-case protection. It enables reformulation into linear programs, preserving the complexity of deterministic models and allowing scalable solutions using standard optimization techniques. Compared to ellipsoidal sets [14], which require second-order or semi-definite programming, the polyhedral approach offers greater tractability [15].

Unlike probabilistic methods that rely on distributional assumptions and often lead to nonconvex or chance-constrained formulations, the polyhedral model guarantees feasibility without stochastic knowledge [16]. It also flexibly captures parameter dependencies, supporting diverse use cases.

To apply localized uncertainty, sensor nodes were partitioned into spatially compact, equally sized groups using the balanced K-Means method, which has demonstrated effectiveness across various domains [17][18]. This structure facilitates region-specific deviation modeling in

underwater network design by minimizing intra-cluster distances while maintaining uniform group sizes.

The balanced K-Means algorithm divides the sensor set N into k clusters of equal size n_i, minimizing intra-cluster variance. At each iteration t, cluster centroids are updated as $C_i(t+1) = \frac{1}{n_i}\sum_{j\in C_i(t)} x_j$. Sensors are then reassigned via a weighted bipartite matching process that minimizes the total squared distance to centroids, subject to $|C_i| = n_i$. This is achieved using a virtual slot index $a \in [1,n]$ with edge weights defined as $W(a,i) = \text{dist}(x_i, C_{(a \bmod k)+1})^2$ for all $i \in [1,n]$ [10].

Unlike standard K-Means, the equal-size constraint introduces global dependencies, requiring iterative reassignments to balance cluster sizes and minimize variance. This ensures a fair and symmetric robustness formulation by avoiding region-specific scaling and simplifying constraints [10][19].

Under this formulation, deviations are restricted to one region at a time. To prevent over-conservatism from overly broad uncertainty sets, we adopt a region-based version of the Γ-uncertainty model [15], enabling tractable and focused robustness without excessive conservatism.

We define the polyhedron of feasible sensing rates as the set of all s_k satisfying $s_k^{\text{nom}} \le s_k \le s_k^{\text{nom}} + s_k^{\text{dev}}$ for each sensor $k \in N$, and for all regions $R_j \in \mathscr{R}$, the sum of sensing rates within R_j satisfies $\sum_{k\in R_j} s_k \le (1+\alpha)\sum_{k\in R_j} s_k^{\text{nom}}$. More explicitly, $\mathscr{U} = \{s_k \in \mathscr{S} : s_k^{\text{nom}} \le s_k \le s_k^{\text{nom}} + s_k^{\text{dev}} \ \forall k \in N;\ \sum_{k\in R_j} s_k \le (1+\alpha)\sum_{k\in R_j} s_k^{\text{nom}} \ \forall R_j \in \mathscr{R}\}$. This formulation allows for individual deviations while controlling aggregate sensing rates regionally, balancing robustness with practical conservatism.

The worst-case realization of the left-hand side in the energy constraint leads to the robust counterpart constraint $\max_{s\in\mathscr{U}} \sum_{k\in N} s_k \cdot a_{ik} \le e_i$, where $\mathscr{U}$ is the uncertainty set defined by the intervals and regional budget constraints, and a_{ik} denotes the energy consumption at node i associated with the sensing activity of node k, represented in the original constraint as $\sum_{(i,j)\in A} Te_{ij}^{\text{TX}} f_{ij}^k + \sum_{(j,i)\in A} Te_{ji}^{\text{RX}} f_{ji}^k$. We now dualize the inner maximization problem. The primal form of this inner maximization is:

$$\max_{s_k} \quad \sum_{k\in N} s_k \cdot a_{ik} \tag{7}$$

$s.t.$

$$s_k^{\text{nom}} \le s_k \qquad \forall k \in N \tag{8}$$

$$s_k \le s_k^{\text{nom}} + s_k^{\text{dev}} \qquad \forall k \in N \tag{9}$$

$$\sum_{k\in N} \beta_{kj} s_k \le (1+\alpha)\sum_{k\in N} \beta_{kj} s_k^{\text{nom}} \qquad \forall j \in \mathscr{J} \tag{10}$$

$$\beta_{kj} \in \{0,1\} \qquad \forall k \in N,\ \forall j \in \mathscr{J} \tag{11}$$

Introducing dual variables $\mu_{ik} \ge 0$ for the upper bounds, $\lambda_{ik} \ge 0$ for the lower bounds, and $\theta_{ji} \ge 0$ for the regional constraints, the dual of this linear maximization becomes:

$$\min_{\mu,\lambda,\theta} \quad \sum_{k\in N} \mu_{ik}(s_k^{\text{nom}} + s_k^{\text{dev}}) - \sum_{k\in N} \lambda_{ik} s_k^{\text{nom}} + (1+\alpha)\sum_{j\in\mathscr{J}} \theta_{ji} \sum_{k\in N} \beta_{kj} s_k^{\text{nom}} \tag{12}$$

$s.t.$

$$\mu_{ik} - \lambda_{ik} + \sum_{j\in\mathscr{J}} \theta_{ji}\beta_{kj} \ge a_{ik} \quad \forall k \in N \tag{13}$$

$$\mu_{ik}, \lambda_{ik} \ge 0 \qquad \forall i \in N, k \in N \tag{14}$$

$$\theta_{ji} \ge 0 \qquad \forall j \in \mathscr{J}, i \in N \tag{15}$$

Consequently, replacing the original constraint with its dual leads to the robust energy constraint. The resulting compact LP model, which represents the robust counterpart of $E_{\max}^{\text{det}}$, is denoted by $E_{\max}^{\text{rob}}$:

$$min \quad e_{\max}^{\text{rob}} \tag{16}$$

$s.t.$

$$\sum_{k\in N} \Big[\mu_{ik}(s_k^{\text{nom}} + s_k^{\text{dev}}) - \lambda_{ik} s_k^{\text{nom}} + \sum_{j\in\mathscr{J}} \theta_{ji}(1+\alpha)\beta_{kj} s_k^{\text{nom}}\Big] \le e_i \qquad \forall i \in N \tag{17}$$

$$e_{\max}^{\text{rob}} \ge e_i \qquad \forall i \in N \tag{18}$$

$$(2), (5), (6), (13) - (15).$$

C. Simulation Model

The simulation framework developed for underwater sensor networks encompasses several critical stages to capture the complex interactions between sensors, underwater vehicles, and the seafloor environment. These stages ensure realistic modeling of detection processes and yield the data generation rate as a key uncertainty parameter to support the accuracy of robust network model.

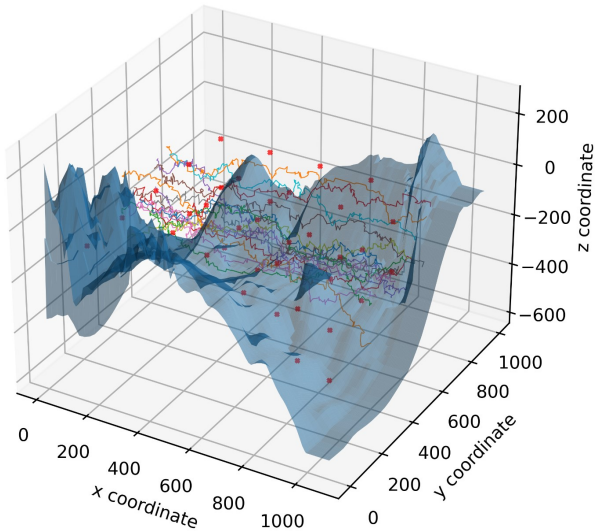

Figure 1. Trajectories of AUVs in 3D underwater environment

The process begins with generating detailed bathymetric maps to accurately characterize the underwater terrain. Underwater vehicles are initialized at random locations, and their trajectories are simulated based on predefined mobility rules formulated to emulate smooth underwater motion. A network of 40 sensors is deployed in a grid-like fashion with terrain-aware feasibility checks and appropriate detection radii to ensure sufficient coverage [20]. Each sensor is assumed to possess both an absolute detection area, which is designed to be tangential to those of

neighboring nodes, and a surrounding probabilistic zone where the likelihood of detection decays with distance due to signal attenuation. This dual-layer sensing model captures detection uncertainty beyond the immediate sensing range, resulting in a more precise representation of sensing behavior.

Sensor detection durations are evaluated over discrete time intervals, integrating continuous environmental monitoring with event-driven sensing triggered by the transitions of underwater vehicles. In each run, a total of 100 underwater vehicles follow their trajectories, during which sensors remain actively engaged in monitoring and record the cumulative durations of the detection process. These values are normalized by the total simulation time to compute individual data generation rates. To account for environmental variability, the process is independently repeated 30 times using different random seeds, and the consistency observed across these repetitions confirms the reliability of the estimated sensing rates used in the optimization model. The modular simulation framework, implemented in Python and conceptually detailed in [6], supports flexible modeling of sensor coverage, AUV mobility, and energy-aware operations, thereby providing a reliable foundation for both current analyses and potential extensions involving more detailed energy models. The energy model adopted in this study is based on the 10-level discrete power scheme described in [21], in which each level defines a communication range along with the corresponding energy cost per bit for both transmission and reception, thereby capturing distance-dependent energy consumption. Figure 1 presents an overview of the simulation environment along with the intruder trajectories.

III. Computational Results

In this section, we present the results of numerical experiments conducted in two main phases. First, we examine the impact of incorporating uncertainty into energy allocation decisions during the configuration phase. Second, we compare the performance of robust and deterministic network designs in terms of operational lifetime once deployed. These analyses aim to evaluate the network's capability to maintain performance when exposed to potential uncertainties after configuration.

In the deterministic model, all parameters are assumed to be known with complete accuracy. In contrast, the robust model takes into account possible deviations in the data generation rate, which is based on event-driven measurements observed throughout the simulation. The maximum battery allocations for both the deterministic and robust models are obtained by solving their respective linear programming formulations, denoted as $E^{\text{det}}_{\text{max}}$ and $E^{\text{rob}}_{\text{max}}$, respectively. The goal in both cases is to minimize the highest amount of energy allocated to any single sensor. As expected, the robust model does not yield a better objective value than the deterministic one, since it is designed to handle more demanding and uncertain conditions. Then, we evaluate the practical performance of both configurations by comparing their optimal results across various cases to assess trade-offs and identify the most effective design strategy.

We performed all computations on a 2.50 GHz machine with 16 GB. The optimization problems were solved by IBM ILOG CPLEX Optimization Studio Version: 20.1.0 under a runtime limit of 720 seconds.

A. Configuration Phase: Maximum Energy Allocation

The aim of this section is to analyze how variations in data generation rates, characterized by different uncertainty sets, affect the maximum battery allocation values (E^{max}) as determined by both the deterministic model ($E^{\text{max}}_{\text{det}}$) and the robust model ($E^{\text{max}}_{rob}$) during the configuration phase. In both models, the default network lifetime is fixed at 100 seconds.

To assess the sensitivity of the robust framework in comparison to the deterministic one, we vary the regional uncertainty budget $\alpha \in \{0.01, 0.05, 0.10, 0.20\}$ within a selected region. Additionally, sensors are allowed to deviate individually by up to three standard deviations (σ) to reflect node-specific uncertainty bounds. For each (α, σ) combination, a robust provisioning is generated to enable lifetime analysis in Section III-B.

These uncertainty parameters determine the level of conservatism in the robust design: larger values lead to broader uncertainty sets, thereby requiring more energy provisioning to guard against adverse scenarios. Although the robust model yields more conservative objective values during the configuration phase, it consistently ensures reliable performance in implementation. In contrast, the deterministic design shows greater performance degradation even under minor deviations.

At this stage, considering the standard deviation bands σ_i (for $i = 1, 2, 3$) with $\sigma_1 < \sigma_2 < \sigma_3$, it is observed that the maximum battery capacity increases against higher σ_j, while all other parameters remain constant. A similar trend is evident across the localized conservativeness levels α_i, though the growth follows a sublinear pattern in percentage terms. This suggests that higher regional conservativeness entails relatively modest additional battery provisioning during the configuration phase, while still ensuring robustness. Although variations in α contribute to the observed gains, the deviation level σ emerges as the primary factor driving regional disparities, as illustrated in Figure 2.

In this context, for the least conservative scenario ($\alpha = 0.05$, σ_1), the average increase in maximum battery allocation under the robust configuration relative to the deterministic baseline is 2.97%. Under the most conservative setting ($\alpha = 0.20$, σ_3), this increase reaches 9.85%.

Region-wise analysis further reveals that sub-region R_1 consistently requires the highest battery allocation, whereas R_3 necessitates the lowest, across all σ levels. This pattern is likely related to the higher sensitivity of critical constraints in R_1 to input deviations. In particular, several nodes in R_1 appear to operate near their feasibility limits. In such cases, even small perturbations can activate binding constraints with high dual values, amplifying their influence on battery provisioning and, in turn, the objective function.

B. Implementation Phase: Network lifetime

This section analyzes the performance of networks designed with both models, as described in Section

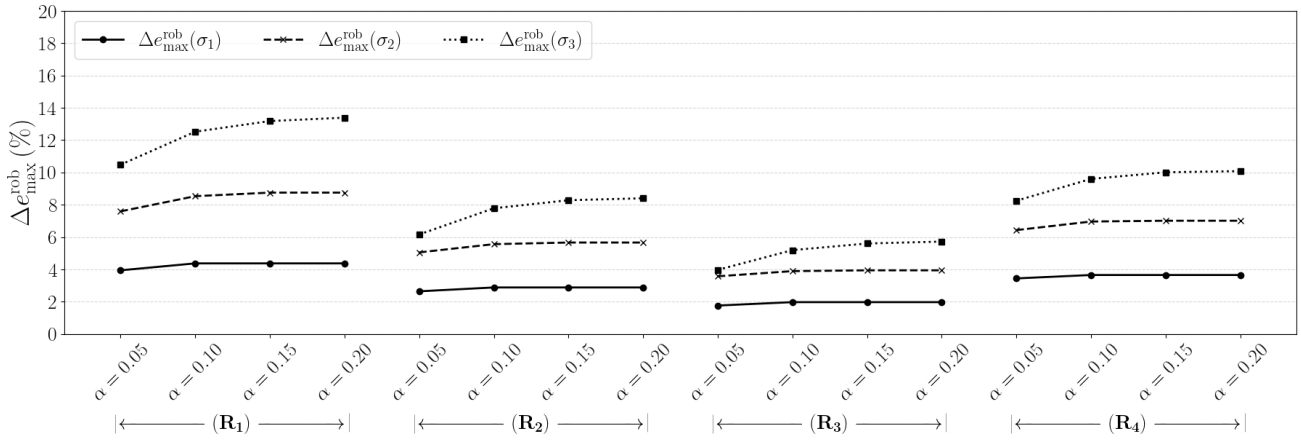

Figure 2. Percentage change of optimal battery capacity across different α and σ values in each sub-region R_j.

III-A, under predetermined parameter combinations. Consequently, given the battery capacities of the sensors and the data transmission paths, the functional duration of each design will be calculated under different data sensing rates and compared with the reference lifetime value T, specified during the design phase. Based on the uncertainty set encompassing the applicable sensing rate vectors for the given network configuration, and for specified values of σ, we generate the set $s' = \{s'_k : k \in N\}$ by selecting sensors whose sensing rates are allowed to deviate from their nominal values and reach the corresponding upper bounds within the predefined sub-regions.

Then, we solve formulations (19) and (21) to determine the lifetime of the deterministic and robust designs in each case, respectively. Herein $f^k_{ij,\text{det}}$ and $f^k_{ij,\text{rob}}$ denote the transmission paths, while e^i_{det} and e^i_{rob} represent the battery capacities obtained by solving E^{det}_{max} and E^{rob}_{max}. Hence, we solve LP models since the only unknowns are T_{det} and T_{rob}.

$$\max\ T_{\text{det}} \tag{19}$$

s.t.

$$\sum_{k\in N}\left[\sum_{(i,j)\in A} T_{\text{det}} e^{TX}_{ij} f^k_{ij,\text{det}} s'_k + \sum_{(j,i)\in A} T_{\text{det}} e^{RX}_{ji} f^k_{ij,\text{det}} s'_k\right] \leq e^i_{\text{det}} \qquad \forall i \in N \tag{20}$$

and

$$\max\ T_{\text{rob}} \tag{21}$$

s.t.

$$\sum_{k\in N}\left[\sum_{(i,j)\in A} T_{\text{rob}} e^{TX}_{ij} f^k_{ij,\text{rob}} s'_k + \sum_{(j,i)\in A} T_{\text{rob}} e^{RX}_{ji} f^k_{ij,\text{rob}} s'_k\right] \leq e^i_{\text{rob}} \qquad \forall i \in N \tag{22}$$

The sensor network is partitioned into four disjoint regions $R_j \subseteq N$ (for $j = 1, 2, 3, 4$), satisfying $\bigcup_{j=1}^{4} R_j = N$ and $|R_j| = 10$ for each j. Deviation bands are applied precisely to the sensors within each active R_j, consistent with the robust configuration. The network lifetime achieved under the robust configuration closely approaches or slightly underperforms the reference lifetime value of 100 seconds across all cases, as observed in Figure 3.

Under nominal conditions, where no deviations occur, higher values of α in the robust configuration extend network lifetimes by provisioning additional capacity. When deviations arise, as illustrated in Figure 3, increased α enhances the model's ability to maintain feasible operation durations and mitigate premature battery depletion. This adaptive behavior is achieved by conservatively allocating battery capacity, selectively restricting the total magnitude of deviations within regions characterized by spatially correlated risks.

Building on this, the analysis based on parameters α and σ highlights the critical importance of incorporating sensing rate variability through robust optimization to enhance network availability and reliability under high uncertainty. For instance, in the baseline scenario with ($\alpha = 0.05$, σ_1), the deterministic configuration exhibits network lifetimes approximately 9.44%, 11.15%, 11.94%, and 11.97% shorter across regions R_1 to R_4, respectively, compared to the robust model. As uncertainty intensifies, reflected by larger α and σ values, these differences increase substantially, reaching reductions of 14.72%, 17.93%, 15.30%, and 21.75% in the most extreme cases. From the α perspective, the robust design closely approaches the reference lifetime under low σ conditions. However, as σ increases, the model requires more conservative allocations to accommodate higher uncertainty, making it more difficult to achieve the reference lifetime. This reflects the inherent trade-off between robustness and performance in the presence of increased variability. Ultimately, region-wise analysis indicates that lifetime variability increases across each region as the levels of α or σ increase.

Together, these findings confirm that the robust design effectively sustains network lifetime close to the reference target despite any considered level of uncertainty, balancing conservatism with operational efficiency.

IV. Conclusion and Future Work

This paper proposes a robust optimization framework for the design of an UWSN focused on target detection, ensuring energy efficiency and network reliability under uncertainty. Utilizing a simulation-based robust optimization framework with real-world bathymetric data, we

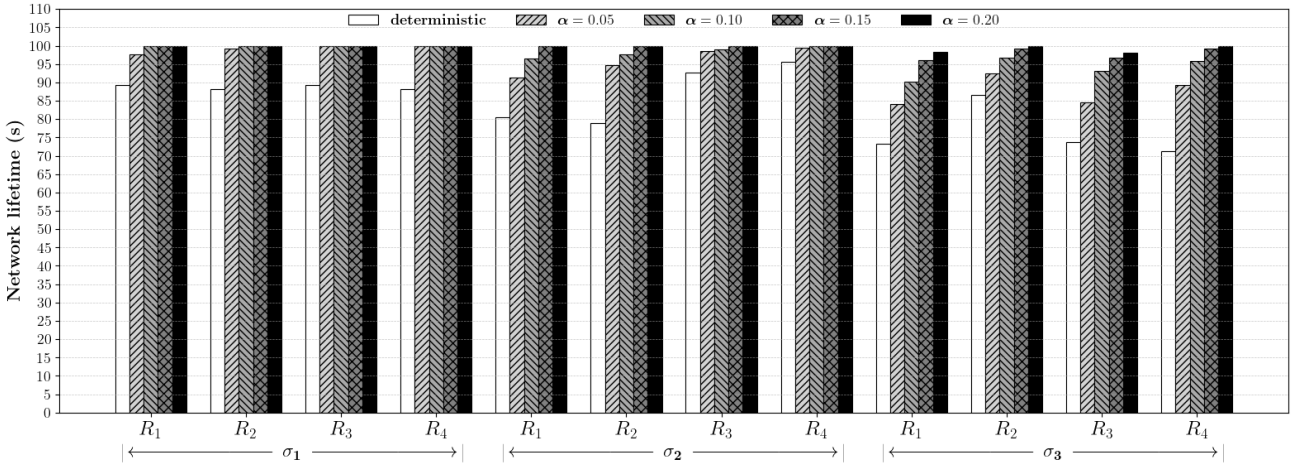

Figure 3. Comparison of deterministic and robust lifetime performance for a 40-sensor network across varying parameters

address uncertainties in sensing rates stemming from both regional and individual sensor deviations, and evaluate their impact on overall network performance. To enhance this framework, we integrate a region-based deviation model that provides a more comprehensive assessment of spatial vulnerabilities across the network.

This study develops an uncertainty set grounded in system-specific data obtained through simulation, leveraging a polyhedral formulation that improves the scalability of the proposed method and enhances its suitability for practical applications.

Results from comprehensive tests indicate that even minimal variations in sensing rates can severely compromise deterministic designs, causing early network failures. In contrast, the robust design consistently delivers sustained long-term performance, substantially exceeding the reliability of deterministic methods, even in the presence of varying regional and localized spatial instabilities.

Following the worst-case scenario implementations that are localized within one of the designated regions, future work may explore more comprehensive deviation models to address increasingly complex and unstructured conditions across networks with varying numbers of sensors. These include sensors deviating outside the active region, mixed-region cases, and over-budget scenarios exceeding the predefined uncertainty limits. Additionally, alternative deployment and partitioning strategies can be employed to evaluate their impact on robustness and enable comparative analyses.

REFERENCES

[1] I. Akyildiz, D. Pompili, and T. Melodia, "Underwater acoustic sensor networks: Research challenges," *Ad Hoc Networks*, vol. 3, no. 3, pp. 257–279, May 2005.

[2] A. F. Harris and M. Zorzi, "Modeling the underwater acoustic channel in ns2," in *Proceedings of the 2nd International Conference on Performance Evaluation Methodologies and Tools*, ser. ValueTools '07, Nantes, France: ICST (Institute for Computer Sciences, Social-Informatics and Telecommunications Engineering), 2007, pp. 1–8.

[3] I. Vasilescu, K. Kotay, D. Rus, M. Dunbabin, and P. Corke, "Data collection, storage, and retrieval with an underwater sensor network," *SenSys 2005 - Proceedings of the 3rd International Conference on Embedded Networked Sensor Systems*, pp. 154–165, Nov. 2005.

[4] E. Felemban, F. Shaikh, U. Qureshi, A. Sheikh, and S. Qaisar, "Underwater sensor network applications: A comprehensive survey," *International Journal of Distributed Sensor Networks*, vol. 2015, pp. 1–14, Nov. 2015.

[5] F. D'Andreagiovanni and A. Nardin, "Towards the fast and robust optimal design of wireless body area networks," *Applied Soft Computing*, vol. 37, pp. 971–982, Apr. 2015.

[6] O. Eren and A. Altin-Kayhan, "A simulation-informed robust optimization framework for the design of energy efficient underwater sensor networks," *Ad Hoc Networks*, vol. 178, p. 103 933, 2025.

[7] K. Kumar Gola, N. Chaurasia, B. Gupta, and D. Singh Niranjan, "Sea lion optimization algorithm based node deployment strategy in underwater acoustic sensor network," *International Journal of Communication Systems*, vol. 34, no. 5, e4723, 2021.

[8] K. Sunil Kumar, D. Singh, and V. Anand, "Strategic node deployment scheme for maximizing coverage area and network lifetime in uasns using voronoi-fuzzy c-means and salp swarm optimization," *IEEE Sensors Journal*, vol. 24, no. 10, pp. 16 926–16 934, 2024.

[9] L. Santoro, D. Brunelli, and D. Fontanelli, "Unveiling the undersea: A collaborative approach to monitoring underwater objects," in *2024 IEEE International Workshop on Metrology for Industry 4.0 IoT (MetroInd4.0 IoT)*, 2024, pp. 76–81.

[10] M. I. Malinen and P. Fränti, "Balanced k-means for clustering," in *Structural, Syntactic, and Statistical Pattern Recognition*, Berlin, Heidelberg: Springer Berlin Heidelberg, Aug. 2014, pp. 32–41.

[11] F. D'Andreagiovanni and A. Nardin, "Towards the fast and robust optimal design of wireless body area networks," *Applied Soft Computing*, vol. 37, pp. 971–982, 2015.

[12] B. Braem *et al.*, "The need for cooperation and relaying in short-range high path loss sensor networks," in *2007 International Conference on Sensor Technologies and Applications (SENSORCOMM 2007)*, 2007, pp. 566–571.

[13] M. R. Bharamagoudra and S. S. Manvi, "Deployment scheme for enhancing coverage and connectivity in underwater acoustic sensor networks," *Wireless Personal Communications*, vol. 89, pp. 1265–1293, 2016.

[14] A. Ben-Tal and A. Nemirovski, "Robust solutions of uncertain linear programs," *Operations Research Letters*, vol. 25, no. 1, pp. 1–13, 1999.

[15] D. Bertsimas and M. Sim, "The price of robustness," *Operations Research*, vol. 52, no. 1, pp. 35–53, 2004.

[16] M. Raayatpanah, T. Weise, J. Wu, M. Tan, and P. Pardalos, "Robust optimization for minimizing energy consumption of multicast transmissions in coded wireless packet networks under distance uncertainty," *Journal of*

Combinatorial Optimization, vol. 46, no. 4, pp. 815–838, Aug. 2023.

[17] Y. Zhang, H. Sun, and J. Yu, "Clustered routing protocol based on improved k-means algorithm for underwater wireless sensor networks," in *2015 IEEE International Conference on Cyber Technology in Automation, Control, and Intelligent Systems (CYBER)*, 2015, pp. 1304–1309.

[18] D. Arthur and P. Date, "Balanced k-means clustering on an adiabatic quantum computer," *Quantum Information Processing*, vol. 20, no. 9, p. 294, 2021.

[19] R. de Maeyer, S. Sieranoja, and P. Fränti, "Balanced k-means revisited," *Applied Computing and Intelligence*, vol. 3, no. 2, pp. 145–179, 2023.

[20] A. Aljughaiman, "Grid deployment scheme for enhancing network performance in underwater acoustic sensor networks," *IEEE Access*, vol. 11, pp. 112 973–112 987, 2023.

[21] M. Cobanlar, H. Yildiz, V. Akram, O. Dagdeviren, and B. Tavli, "On the trade-off between network lifetime and k-connectivity based reliability in uwsns," *IEEE Internet of Things Journal*, pp. 24 444–24 452, Jul. 2022.